Paper

Autonomous Flight Control for a Large-Scale Unmanned Helicopter
– System Identification and Robust Control Systems Design –

Member	Shuichi Adachi	(Utsunomiya University)
Member	Seiji Hashimoto	(Oyama National College of Technology)
Non-member	Gou Miyamori	(Kawada Industries, Inc.)
Non-member	Anzhong Tan	(Kawada Industries, Inc.)

Conventional unmanned helicopters are used to spray agricultural chemicals and take aerial photographs. In the near future, the aircrafts are expected to be used for a wide array of activities, such as rescuing and fire fighting. Then, an autonomous flight using several sensors typified by a global positioning system (GPS) is highly expected. In this paper, first, system identification experiments for a large-scale unmanned helicopter are carried out to obtain a numerical model of aircraft dynamics. The attitude error of the helicopter is compensated by a stability augmentation system that permits the experiments during the flight. System identification results are shown on the dynamics using the measured input and output data. Next, the position control systems based on the $\mathcal{H}_\infty$ control theory is constructed by using the identified model. Finally, the position control experiments suggest that the proposed modeling and design approach is effective enough for practical applications.

Keywords: unmanned helicopter, autonomous flight, system identification, robust position control

1. Introduction

Recently, unmanned helicopters, particularly large-scale ones, have been expected not only for the industrial fields such as agricultural spraying and aerial photograph, but also for such fields as observation, rescuing, and fire fighting. For these monotonous or dangerous missions, an autonomous flight control of the helicopter is indispensable. The autonomous flight control requires integrating technologies such as trouble diagnosis and obstacle avoidance as well as attitude and position controls.

The flight control of the helicopter involves some difficulties due to the following;

(1) The dynamics of the helicopter are essentially unstable.
(2) The characteristic values in the dynamics are usually nonlinear with air speed.
(3) The helicopter has six degrees of freedom in its motion (up/down, fore/aft, right/left, rolling, pitching, yawing).
(4) The helicopter is a multi-input multi-output system.
(5) Flight modes are cross-coupled.
(6) The flight is strongly affected by disturbances such as wind, temperature, etc.

The helicopter, however, can be modeled as a linear system around trim points, i.e., a flight with no accelerations and no moments. Moreover, the system can be stabilized by using a stability augmentation system (SAS), which can also reduce the influence of cross-couple terms. Therefore, the flight control of the unmanned helicopter with SAS is possible around the trim points. Several unmanned helicopters have been developed [1], [2], or are under development throughout the world. However, a complete autonomous flight control system has not yet been realized.

The goal of the research is to design an autonomous flight control system of a large-scale unmanned helicopter. The authors, at first, carry out the system identification experiments of the full-scale unmanned helicopter (named RoboCopter) to derive the mathematical model. Using the measured input and output data, the dynamics of the helicopter is identified. Then the position control experiments are investigated to show the applicability of the identified models to the position control for the autonomous flight.

2. A Large-Scale Unmanned Helicopter

The configuration of an autonomous flight control of a large-scale unmanned helicopter is shown in Fig. 1. The flight control of the body is accomplished by using various sensors, which are represented by a global positioning system (GPS), in accordance with the command reference transmitted by the ground station. The signals that lack for the autonomous flight can be estimated by the on-board digital signal processor (DSP). The control algorithm for the flight is installed in the DSP in advance. Thus the unmanned helicopter can be remotely controlled on the ground station. This experiment is devised so that a remote operator can transmit a rudder modification signal directly to the

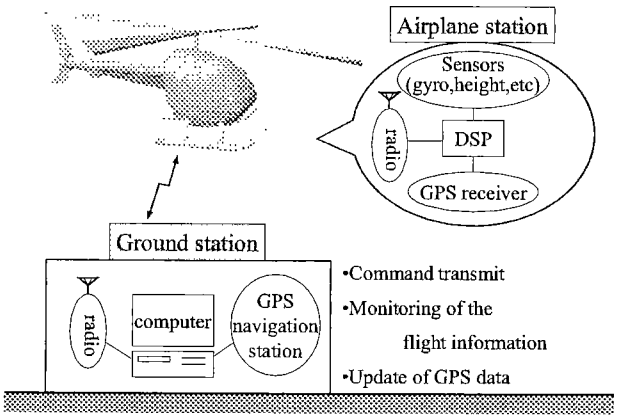

Fig. 1. Configuration of an autonomous flight system.

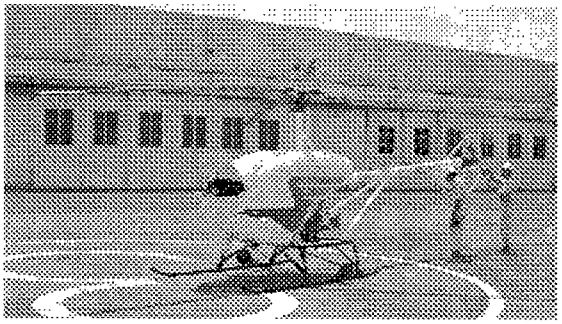

Fig. 2. The experimental large-scale unmanned helicopter named RoboCopter.

Table 1. Size and performance of RoboCopter

body dimensions	length	7.31 m
	width	1.99 m
	height	2.65 m
weight	total weight	794 kg
	empty weight	500 kg
	payload	294 kg
engine	type	air-cooled 4-cycle engine
	power	124 kW(168HP)
main rotor	number of blades	3
	diameter	8.18 m
tail rotor	number of blades	2
	diameter	1.30 m
continuous flight time	100 min (extendable to 4 h depending on payload)	

flight control in order to keep the flight safe.

The full-scale unmanned helicopter (RoboCopter) developed by Kawada Industries, Inc. [3] is shown in Fig.2. The size and performance of the helicopter are summarized in Table 1. This unmanned helicopter is a remodeled version of a manned helicopter, Shweizer 300CB. The flight time can be extended from 100 to 240 min. at the cost of payload. In addition, stabilization of the helicopter is realized by the SAS installed in the DSP.

3. System Identification Experiments

3.1 Nomenclature Figure 3 shows the coordinates to describe the motion of the helicopter. The origin of the helicopter axes is placed on the center of gravity. The variables, constants and terms in the figure

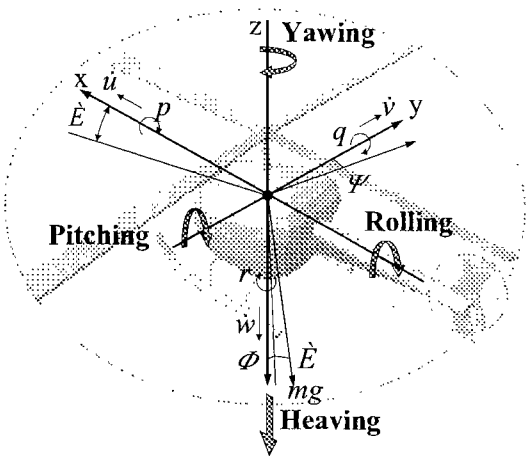

Fig. 3. Helicopter coordinates.

are defined as follows;

x, y, z : aircraft fixed coordinates
p, q, r : angular velocities around x, y, z-axes
x, y, z : positions in x, y, z directions
u, v, w : velocities in x, y, z directions
Φ, Θ, Ψ : roll, pitch, yaw angles
θ_C : lateral cyclic pitch angle
θ_S : longitudinal cyclic pitch angle
θ_{0T} : tail rotor pitch angle
θ_{0M} : main rotor collective pitch angle
m : mass of helicopter
g : gravitational acceleration

rolling : A rotational motion around the x-axis of the body which occurs by changing θ_C

pitching : A rotational motion around the y-axis of the body which occurs by changing θ_S

yawing : A rotational motion around the z-axis of the body which occurs by changing θ_{0T}

heaving : A linear motion in the z-axis direction of the body which occurs by changing θ_{0M}

Each motion is not independent of θ_C, θ_S, θ_{0T}, and θ_{0M}, so there exists a cross coupling. For example, the heaving motion is coupled to the yawing motion [1].

3.2 System Identification Experiments The block diagram of the helicopter compensated by the SAS controller is shown in Fig.4. The command references, which are made in the computer on the ground station are transmitted to the helicopter. Modification rudder signals from the remote operator are added to these command reference and then fed to the SAS controller for the attitude control. These input signals $\theta_C^*, \theta_S^*, \theta_{0T}^*$ and θ_{0M}^* drive rolling, pitching, yawing and heaving motions, respectively. The superscript (*) represents the reference value of those signals. $\theta_C^*, \theta_S^*, \theta_{0T}^*$ and θ_{0M}^* are used as input signals for system identification. In this case, taking the cross-couplings into consideration, each motion was separately excited by the signals. The pseudo random binary signal (PRBS) was applied to a motion of interest, and the constant signals were applied to the other three motions. The sampling time for the experiment was 0.02 s, and the clock period

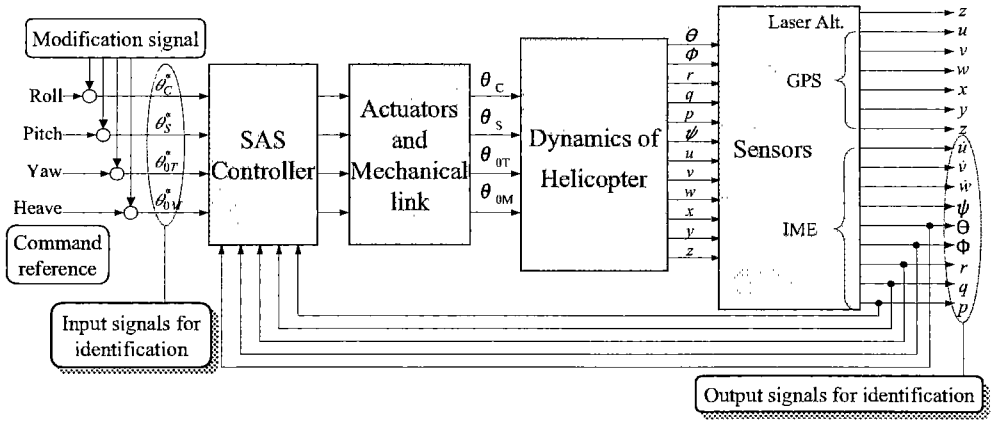

Fig. 4. Construction for system identification experiments on the helicopter with SAS.

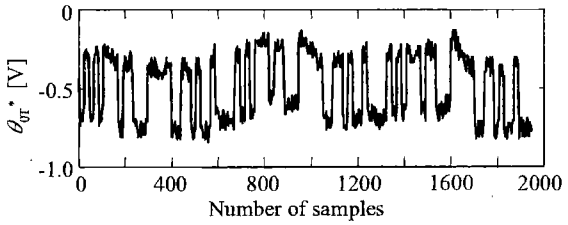

Fig. 5. Input signal (yawing).

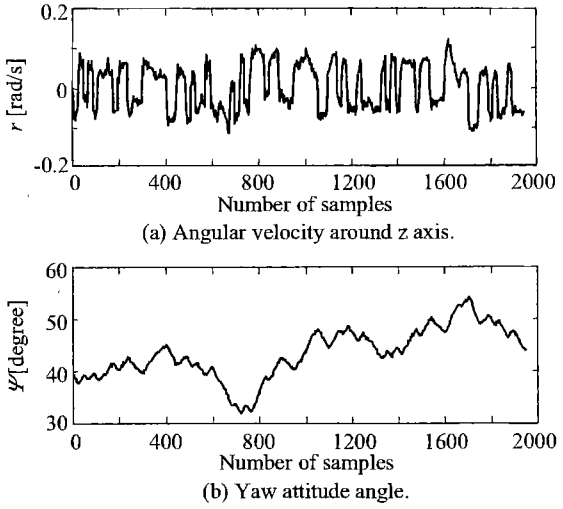

Fig. 6. Output signals (yawing).

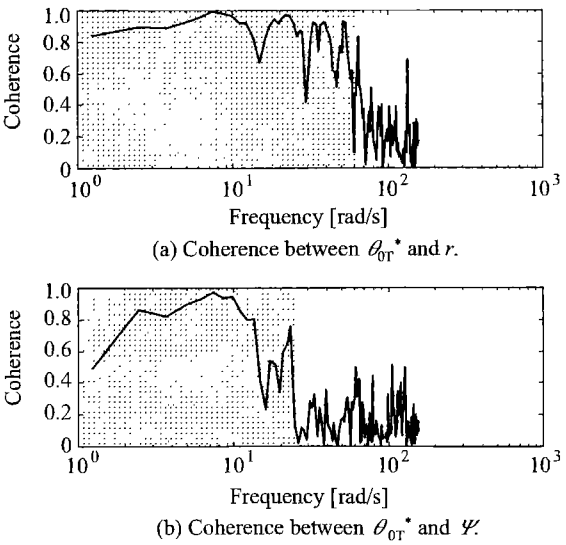

Fig. 7. Coherences for yaw excitation.

of the input was 20 times of the sampling time. The period of the PRBS was 31. The outputs measured by the inertial measurement equipment (IME), which includes gyro system, were: attitude angles (Φ, Θ, Ψ), their angular velocities (p, q, r) and accelerations $(\dot{u}, \dot{v}, \dot{w})$. Velocities (u, v, w) and positions (x, y, z) were measured by GPS, and height (z) by a laser distance meter. The signals $p, q, r, \dot{u}, \dot{v}, \dot{w}, \Phi, \Theta$ and Ψ, which directly influence the control design for the autonomous flight, were selected as output signals for system identification.

As an example, motion about yawing excitation is described below. The measured input and output signals are shown in Figs.5 and 6, respectively. As can be seen in Fig.6, it is verified that the output signals r and Ψ, which are strongly related to a yawing motion, are excited by θ_{0T}^*. The coherences between the input θ_{0T}^* and the outputs r and Ψ, which indicate how well θ_{0T}^* corresponds to r and Ψ at each frequency, are shown in Fig.7. The accurate identification can be expected at the frequency range where the coherences are close to 1, that is shaded in Fig.7.

4. System Identification

Using measured input-output data, the system identification based on the prediction error method is applied to the helicopter as a single-input single-output (SISO) system. The number of data was 1,950. The auto-regressive with exogenous input (ARX), auto-regressive moving average with exogenous input (ARMAX), output error (OE) and Box-Jenkins (BJ) models [4] were used to describe the dynamics of the helicopter. The cross-validation was utilized to determine the order of the ARX model, and then applied the order for the other models as well. Two thirds of the data were used for the identification, and the rest was used for valida-

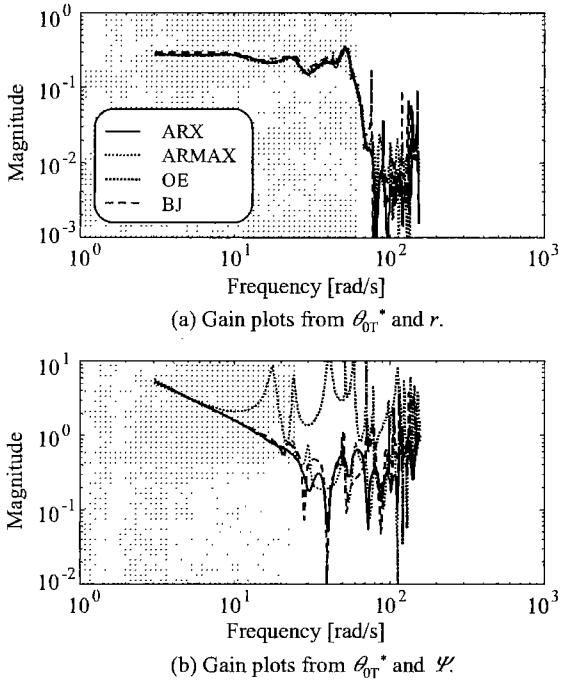

Fig. 8. Identified gain plots by various models for yaw excitation.

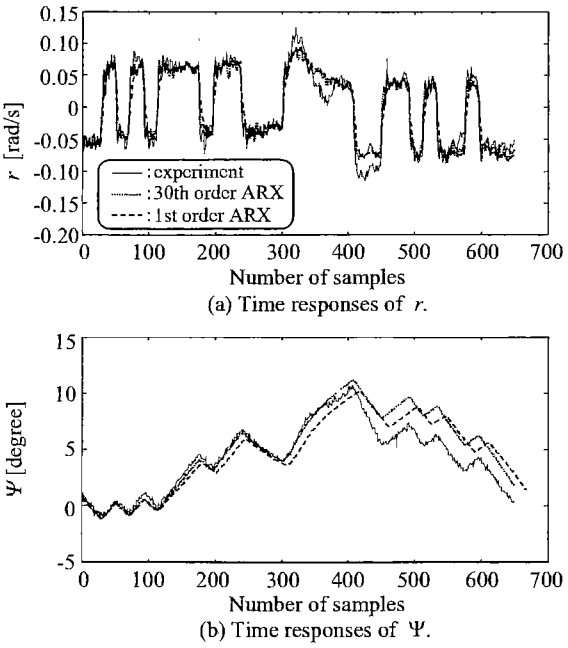

Fig. 9. Time responses of ARX model to yaw excitation.

tion. The model order that can minimize a loss function was 30th with two delays.

Figure 8 shows identified gain plots from θ_{0T}^* to r and Ψ, which are relating variables to the yawing motion. As can be seen in Fig.8, the deviation among these four gain plots is small enough at the frequency range less than 60 rad/s for r/θ_{0T}^*. In case of Ψ/θ_{0T}^*, gain plots except OE model one agree well at the frequency less than 20 rad/s, which falls in the range of a position control. Therefore, the frequency responses of the yawing motion can be identified with high accuracy at that frequency range. It is also well known that the rigid body dynamics are dominant at that frequency range.

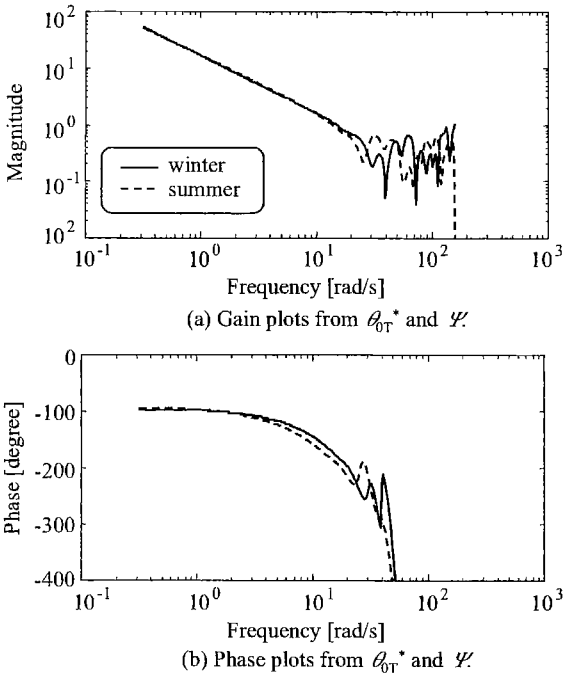

Fig. 10. Comparison of the magnitude (Ψ/θ_{0T}^*) for winter and summer seasons.

Next, to evaluate the identified model in time domain, the remaining one third of input data is applied to the identified ARX model. From the viewpoint of dominant rigid body dynamics, the identification is applied not only to the 30th-order model, but also to the 1st-order ARX model. Figure 9 shows time responses of the model outputs and the measured experimental outputs. From Fig.9, it is confirmed that the model output coincides well with the measured output. Therefore, the identified model well describes the yawing motion of the experimental helicopter.

A change of the helicopter dynamics against the environment such as seasonal changes will be discussed. Since the above data was measured in winter, different experiments were accomplished in summer. The identified gain plots of the yawing dynamics (Ψ/θ_{0T}^*) for both winter and summer seasons are compared in Fig.10. The magnitude for winter agrees with the summer season's values at the frequency range where the coherence is close to 1. Therefore, it can be concluded that the seasonal change of dynamics is not critical under the bandwidth less than 20 rad/s in control.

5. Position Controller Design

In this section, the design problem of position control for an autonomous flight by using the identified model is focused. The controller concerns a yawing motion of the helicopter is designed based on the $\mathcal{H}_\infty$ control theory [5].

The design specifications for the yawing motion are

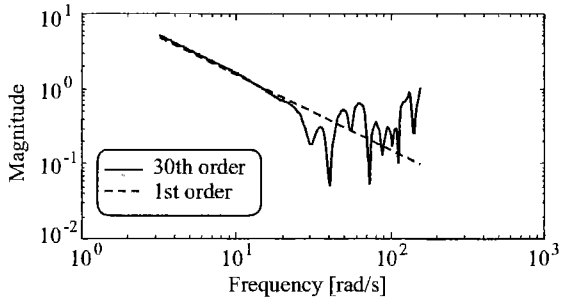

Fig. 11. Gain plots of P(solid line) and P_n(dashed line).

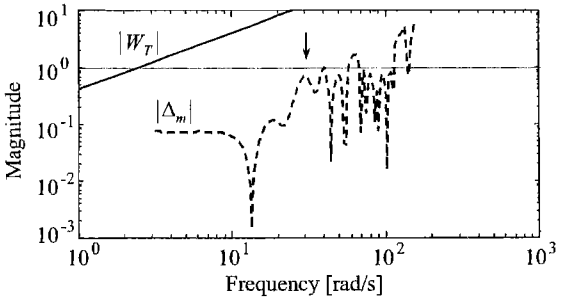

Fig. 12. Gain plots of Δ_m(dashed line) and W_T(solid line).

the followings;

(S1) Steady-state error and overshoot are less than 5 degree.

(S2) It is possible to track the ramp reference signal.

(S3) Settling time is less than 2 s.

The first specification is defined relating to the accuracy of a magnetic compass. The second and the third specifications are defined from the viewpoint of the applied force which does not result in a mechanical damage somewhere in a body. In this case, yaw rate of reference signal is limited to 90 degree per 5 s.

In this design procedure, it can be assumed that the model using the identified 30th-order model(Ψ/θ^*_{0T}) shown in Fig.8(b) is the real experimental plant P, and the model using the identified 1st-order model is the nominal plant P_n. Figure 11 shows the gain plots of P and P_n. Then, the multiplicative uncertainty Δ_m, which is derived from $\Delta_m = (P - P_n)/P_n$, is shown in Fig.12. It is clear that the limitation of the bandwidth for the position control is less than 20 rad/s because of its zero-cross frequency. Taking limitation into account, the weighting function W_T for the complementary sensitivity function $T := PC/(1+PC)$, C is the controller transfer function, is selected to satisfy the restriction $|\Delta_m| < |W_T(j\omega)|, \forall\omega$, by

$$W_T(s) = \frac{s/0.25 + 1}{10} \quad \cdots\cdots\cdots\cdots\cdots\cdots (1)$$

The gain plot is also shown by solid line in Fig.12. In this figure, the bandwidth is selected at 2.5 rad/s which can satisfy the specification (S3).

According to the weighting function W_S for the sensitivity function $S := 1/(1+PC)$, it is recommended to be the double integrator in order to satisfy the specifications (S1) and (S2) as the following, since its dynamics are directly reflected in the $\mathcal{H}_\infty$ controller.

$$W_S(s) = \frac{2.59}{s^2} \quad \cdots\cdots\cdots\cdots\cdots\cdots\cdots\cdots (2)$$

The generalized plant including these weighting functions is illustrated in Fig.13. As a result of these weighting functions, the $\mathcal{H}_\infty$ controller of the 2nd-order which includes the single pole-zero cancellation at $s = 0$ can be obtained as

$$C(s) = \frac{3.30 \times 10^3 (s + 1.04)}{s(s + 1.98 \times 10^4)} \quad \cdots\cdots\cdots\cdots\cdots (3)$$

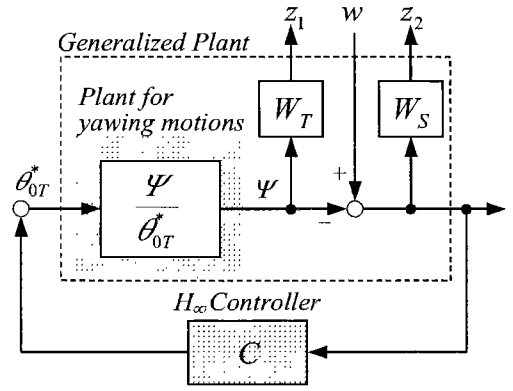

Fig. 13. Generalized Plant.

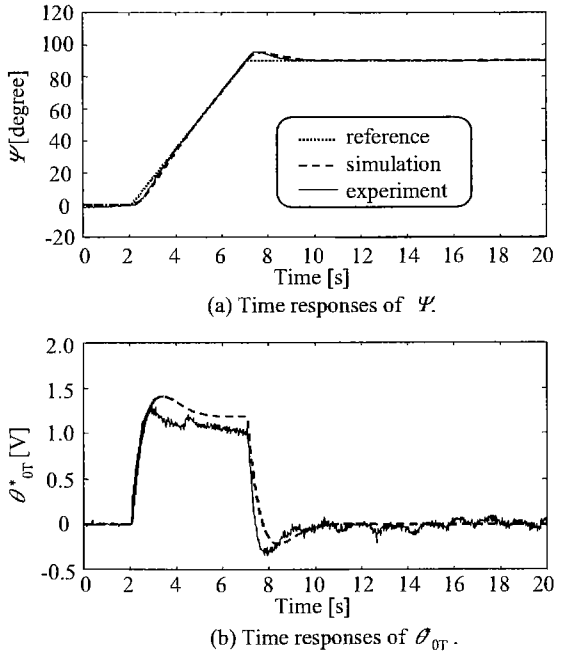

Fig. 14. Time responses to ramp position reference signal.

6. Experimental Implementation

In order to examine the robust stability and the control performance of the system, a ramp position reference signal, 90 degree per 5 s, to the yawing control system has been applied. Figure 14 shows the time re-

sponses of the yaw angle Ψ and the control input θ_{0T}^{*}. It can be concluded that the robust control can be performed by the $\mathcal{H}_\infty$ controller not only to stabilize the system but also to follow the reference with satisfying the specifications.

7. Conclusion

System identification experiments were applied to the large-scale unmanned helicopter compensated by SAS. The modeling by system identification was done through numerical analysis using the measured data.

We have also focused on the design procedure of position control system based on the $\mathcal{H}_\infty$ control by using the identified model and investigated the position control experiments. The effectiveness of the proposed modeling and the design approach for an autonomous flight have been experimentally confirmed .

(Manuscript received April 2, 2001)

References

(1) H. T. Nguyen and N. R. Prasad, "Fuzzy Modeling and Control -Selected Works of M. Sugeno," Chapter 2, CRC Press, 1999.

(2) Y. Kobayashi and K. Liu, "Modeling and Robust Control of A Single-Rotor Helicopter," *Proc. of SICE 26th Control Theory Symposium*, pp. 111-116, 1997 (in Japanese).

(3) G. Miyamori, Q. Zhao, M. Nakamura, A. Tan, K. Akachi and M. Hirai, "Development of An Unmanned Multipurpose Utility Helicopter(RoboCopter)," *Proc. of 35th Aircraft Symposium of JSASS*, pp. 89-92, 1997 (in Japanese).

(4) L. Ljung, " System Identification -Theory for the User (2nd edition)," Prentice Hall, Englewood Cliffs, NJ, 1999.

(5) J. C. Doyle, K. Glover, P. P. Khargonekar and B. A. Francis, " State-Space Solutions to Standard $\mathcal{H}_2$ and $\mathcal{H}_\infty$ Control Problems," *IEEE Trans. on Automatic Control*, Vol. 34, No. 8, pp. 831-847, 1989.

(6) A. Tan, T. Kawada, A. Azuma, S. Saito and Y. Okuno, "Theoretical and Experimental Studies on System Identification of Helicopter Dynamics," *Proc. of 20th European Rotorcraft Forum-Amsterdam*, pp. 86.1-86.16, 1994.

(7) M. B. Tischler and M. G. Cauffman, "Frequency-Response Method for Rotorcraft System Identification," *Journal of the American Helicopter Society*, Vol. 37, No. 3, pp. 3-17, 1992.

(8) B. Etkin and L. D. Reid, "Dynamics of Flight (3rd edition)," John Wiley & Sons, Inc., 1996.

(9) S. Hashimoto, T. Ogawa, S. Adachi, A. Tan and G. Miyamori, "System Identification Experiments on a Large-Scale Unmanned Helicopter for Autonomous Flight," *Proc. of IEEE International Conference on Control Applications(CCA2000)*, pp.850-855, 2000.

Shuichi Adachi (Member) He was born in Kanagawa Prefecture, Japan, on October 19, 1957. He received the B.E., M.E. and Ph.D. degrees in Electrical Engineering from Keio University, Yokohama, Japan, in 1981, 1983, and 1986, respectively. From 1986 to 1990, he was employed by Toshiba Research and Development Center. Since 1990, he has been an associate professor in the Department of Electrical and Electronic Engineering, Utsunomiya University. His current research interests include system identification theory and its application to real systems. Dr. Adachi is a member of the IEEE, the Society of Instrument and Control Engineers, and the Japan Society of Mechanical Engineers.

Seiji Hashimoto (Member) He was born in Aomori Prefecture, Japan, on December 19, 1971. He received the B.E. M.E. and Ph.D. degrees in Electrical and Electronic Engineering from Utsunomiya University, Tochigi, Japan, in 1994, 1996 and 1999, respectively. From 1999 to 2000, he was a researcher at Satellite Venture Business Laboratory, Utsunomiya University. Since 2000, he has been a research associate in department of mechanical engineering, Oyama National College of Technology. His interests include modeling, motion control, vibration control, and flight control. Dr. Hashimoto is a member of IEEE IAS, CSS, the Society of Instrument and Control Engineers, and the Japan Society of Mechanical Engineers. He received the IEEJ Paper Presentation Award in 1996.

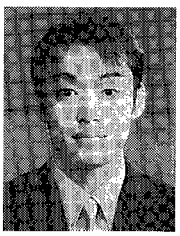

Gou Miyamori (Non-member) He was born in Hiroshima Prefecture, Japan, on July 30, 1970. He received the B.E. and M.E. degrees in Aeronautical Engineering form Kyushu University, Fukuoka, Japan, in 1993 and 1995, respectively. Since then he has been working on unmanned helicopters for Kawada Industries, Inc.. His interests include flight control and flight test. Mr. Miyamori is a member of the Japan Society for Aeronautical and Space Sciences, and the American Helicopter Society.

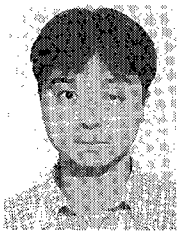

Anzhong Tan (Non-member) He was born in Chongqin, China, on January 13, 1962. He received the B.E., M.E., and Ph.D. degrees in Aeronautical Engineering from Kyushu University, Fukuoka, Japan, in 1984, 1986 and 1989, respectively. Since 1991, he has been working for Kawada Industries, Inc., Japan as an R&D manager. His interests include helicopter aerodynamics and flight control, noise and vibration reduction, etc. Dr. Tan is a member of the Japan Society for Aeronautical and Space Sciences, and the American Helicopter Society.